

Surface Temperature Estimation from Landsat ETM⁺ Data for a part of the Baspa Basin, NW Himalaya, India

K. Babu Govindha RAJ¹ and Kevin FLEMING²

¹ National Remote Sensing Agency (NRSA)

Balanagar, Hyderabad-500 037

Andhra Pradesh, India

² Department 2.1 Physics of the Earth

GeoForschungsZentrum Potsdam

Potsdam, D-14473, Germany

(Received May 17, 2007; Revised manuscript accepted September 11, 2007)

Abstract

This paper presents results of extracting surface temperatures from Landsat ETM⁺ Thermal Band (Band 6, Low gain) data for the Baspa River Basin, Himachal Pradesh, India. Initially, Top of Atmospheric (TOA) radiance is extracted from the digital number (DN) values. The TOA radiance is then converted to surface radiance by applying the Reference Channel Emissivity (RCE) method, assuming the emissivity of the study area is constant (0.97, the emissivity of glacier ice). The surface temperature is then extracted from the surface radiance. Based on images from June and October 2000, mean temperatures of 17.25°C and 11.98°C, respectively, are inferred. The extracted temperature data were compared to observed temperatures and showed a good correlation, with differences of 1–2°C.

1. Introduction

Advances in space technology has increasingly allowed the use of satellite data to study complex physical processes on the Earth's surface. In the field of glaciology, various types of remote sensing studies have been successfully undertaken, including examining the movements of glaciers using radar interferometry (Rignot and Kanagaratnam, 2006), and detecting changes in the duration and onset of the ablation season (*e.g.* Smith *et al.*, 2003). In Himalaya, glacier retreat and mass balance assessments using the accumulation area ratio (AAR) method have been attempted. (Kulkarni *et al.*, 2004; Kulkarni *et al.* 2005). While the mapping of glaciers, retreat of one of the glaciers in the Baspa basin using remote sensing has also been demonstrated (Philip and Sah, 2004).

The Himalaya is one of the youngest mountain systems on Earth, and has a direct influence on the climate, hydrology and environment of the Indian subcontinent. It has the largest concentration of glaciers outside the polar regions, which covering about 31000 km² area and provide glacier stored water to the great Indian rivers, the Ganges, Indus and Brahmaputra. Between these three basins, the Indus basin con-

tains the largest concentration of glaciers (3538), followed by the Ganges (1020) and Brahmaputra (662) (WWF, 2005). Glaciation has occurred in the Himalaya over the last 2 million years, with recent studies indicating about 21 glacial periods alternating with warmer interglacial periods (Raina, 2005).

Today, in the Himalayan region glaciers are distributed in different climatic zones. The mean daily air temperature is low in the month of January and rises during the pre-monsoon period (February to May), with maximum average daily temperatures during late May and early June, while during the post-monsoon (October to January) season, mean daily air temperature decreases. The Himalaya cause changes in the air masses crossing the region, resulting in a special microclimate in the region. The southern plains possess sub-tropical climate with the middle hills having a temperate climate and an alpine climate in the high mountain ranges. The mean level of glaciation varies from 4000 to 5000 m above mean sea level (m.s.l.). The Himalayan glaciers vary in form from niche, cirque, simple-basin and compound-basin glaciers. Glaciers in the Himalayas differ from their counterparts in other parts of the world being high dirty and debris covered in the ablation area. The snout region is usually marked by the formation of an

ice cave.

Glaciers are highly sensitive to climatic fluctuations and are indicators of global warming (Dyrugerov, 2003). During the 20th century, the global mean surface air temperature was increased by ca. 0.6°C (IPCC, 2001), and many small glaciers were retreated considerably. Kaser *et al.* (2006) have proposed, from an assessment of available mass balance data, that the contribution to global sea-level rise by glaciers and ice caps (excluding those associated with Greenland and Antarctica) has been of the order of $0.43 \pm 0.19 \text{ mm a}^{-1}$ between 1961 to 2004, with a value of $0.64 \pm 0.22 \text{ mm a}^{-1}$ for between 1991 to 2004, a period better served by satellite observations. As global warming continues, there will be a shift in the zero temperature line (or snow line) towards higher altitudes, resulting in less input (accumulation) to a given glacier's mass during summer, with increased liquid precipitation, causing further retreat of glaciers and increasing the potential for flooding downstream.

Over the past decade, climate change has had a significant impact on the mountain glaciers and perennial water systems of India, with the increase in global temperature and the resulting enhanced energy exchange between the atmosphere and snow leading to an increase in the rate of glacier retreat in the Himalaya (Kulkarni and Bahuguna, 2002a). It is therefore in the study of the rugged and inaccessible terrain of the Himalaya that satellite remote sensing has proven its usefulness (Kulkarni, 1991; Philip and Ravindran, 1998). A study carried out in the Chandra river basin, Himachal Pradesh, showed that the Samudra Tapu Glacier had receded by 741 m during the 38

year period between 1962 and 2000 (Kulkarni *et al.*, 2006). Making use of satellite stereo data of the 8 glaciers in the Baspa Basin, the Shaune Garang Glacier was found to have retreated 923 m between 1962 and 1998, while investigations carried out in the same region using observations from the Indian Remote Sensing Satellites (IRS) suggest an increase of 75% in stream run-off from 1966 to 1992, with the increase in stream run-off from 1980 correlating with the average global temperature rise (Kulkarni *et al.*, 2002b).

Surface temperature is one of the most important parameters for estimating the effect of climatic change on glaciers. Unfortunately, estimating surface temperature using traditional weather-station based meteorological observations is not a feasible solution for a terrain like the Himalaya. Therefore, through remote sensing studies, a synoptic view of the Himalayan region can be established, and used for regional climatological studies. In this paper, an attempt has been made to estimate the surface temperature of the Baspa Basin from Landsat ETM+ thermal band data (Band 6, Low gain, 10.31 to 12.36 μm , having 30 a m resolution). The features of ETM+ Thermal bands suggest that the low-gain state is useful for retrieving temperatures within the range of 130–350 Kelvin (Barsi *et al.*, 2003b). The extracted surface temperature data was compared with observed temperatures from Sangla observatory.

2. Study Area and Data Used

2.1 Study Area

In the present study, the Baspa river basin, lo-

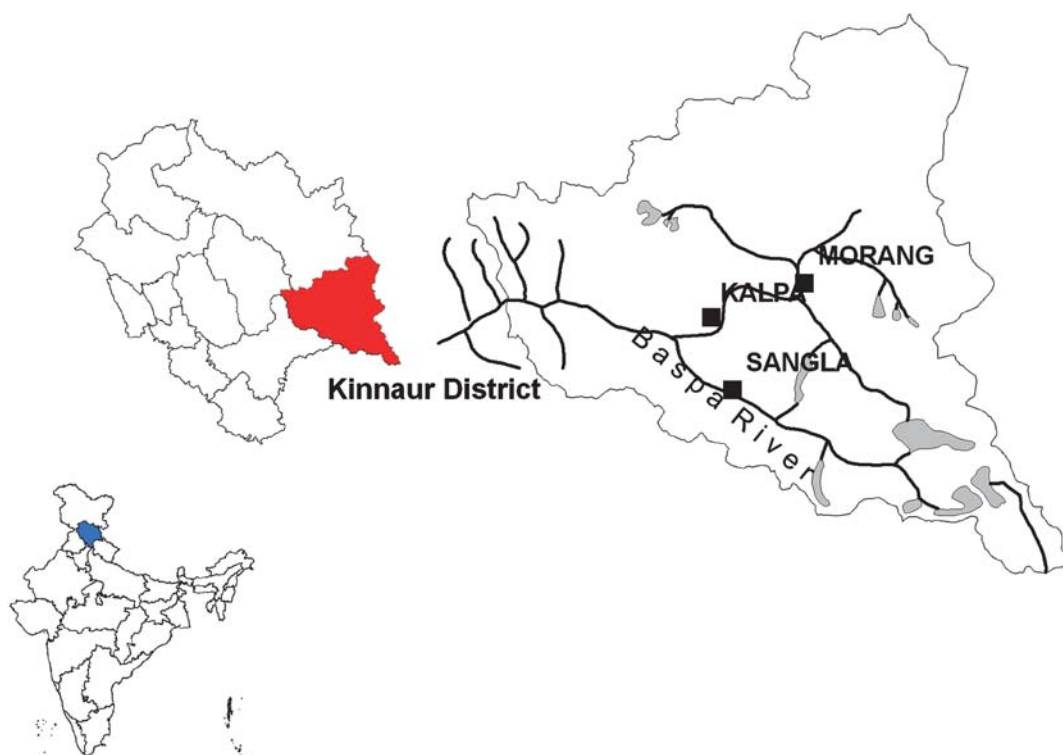


Fig. 1. Location map of the study area.

cated in the Kinnaur District of Himachal Pradesh State, India (Figure 1) has been selected. The Baspa river is a major tributary of the Satluj river, which drains the eastern part of Himachal Pradesh. The river originates at Arsomang and Baspa Bamak glaciers and travels 72 km through the valley before joining the Satluj river at Karcham. The basin is comprised of 19 valley glaciers that vary in form from simple to compound glaciers of varying sizes. The main glaciers of the Baspa valley are Baspa Bamak, Shaune Garang, Joya Garang and Karu, which are situated between altitudes of 4000 m to 6000 m above msl. (Kulkarni *et al.* 2004).

2.2 Data Used

Landsat-7 ETM+ data was used in this study. The multi data sets were acquired on 02-June-2000 (Figure 2a) and 08-October-2000 (Figure 2b), and represent the monsoon and post-monsoon seasons, respectively (Table 1). They consist of Band 6, Low gain Thermal Infra-red data, and were obtained from the GLCF University of Maryland website (<http://glcfapp.umiacs.umd.edu:8080/esdi/>) in GeoTIFF format, and are in the UTM Zone 44 N projection and WGS 84 datum. The surface temperature data was provided by Himachal Pradesh State Electricity Board (HPSEB) meteorological observatory at Sangla.

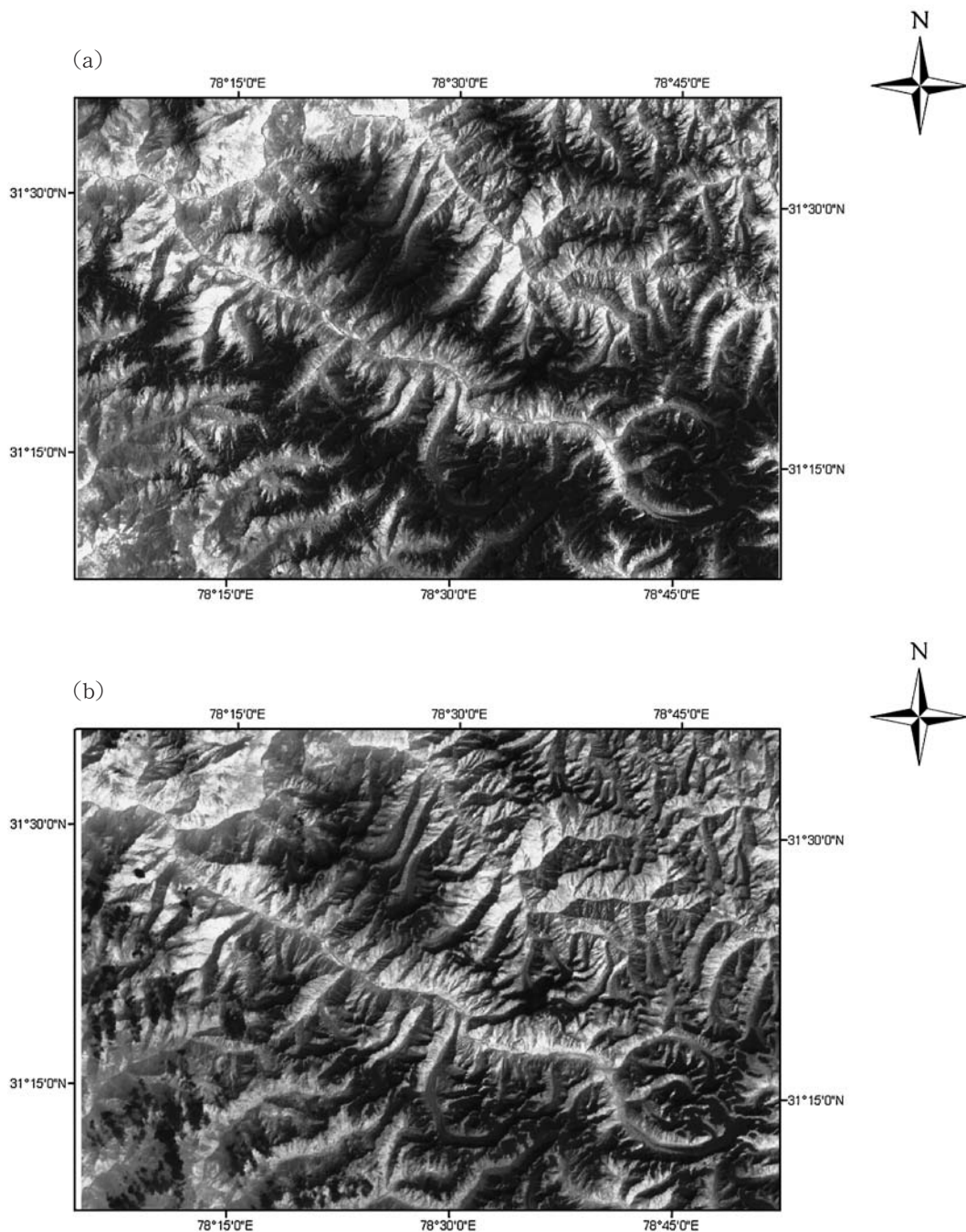


Fig. 2. Landsat ETM+ Band 6 (Low gain) images of the Baspa Basin from (a) 02-June-2000 and (b) 08-October-2000 (see Table 1).

Table 1. Landsat scenes used in the study

Sensor/Band	Acquisition Date	Path/Row	Acquisition Time (start time in GMT)	Sun Elevation	Sun Azimuth
ETM+Band 6 (Low gain)	02-June-2000	146-38	05: 09: 44.0143	67.14	108.80
ETM+Band 6 (Low gain)	08-Oct-2000	146-38	05: 08: 12.8903	47.18	148.064

3. Methodology

The surface properties of snow/ice can be easily observed in the long wave length portion of the electromagnetic spectrum, since snow is almost an ideal blackbody. The strong absorption by snow in the infrared region allows the calculation of the surface temperature of snow from satellite thermal channels. A reflectance spectrum of snow and ice surfaces is shown in Figure 3 (Hall, *et al*, 1985). The infrared radiance measured from a satellite can be converted to surface radiance by applying the Reference Channel Emissivity (RCE) method. The surface radiance is then converted to surface temperature. The methodology followed is schematically shown in Figure 4. The two ETM+Band 6 (Low gain) scenes were processed using the ENVI 4.0 Software.

Due to the lack of field observations in the region, the retrieved surface temperature could only be validated with measured surface temperature from one field site, the Sangla observatory. National Center for Environmental Prediction (NCEP) modelled surface temperatures were also used to validate the retrieved surface temperatures.

3.1 DN to TOA Radiance

The digital number (*DN*) of the Band 6 (low gain) data is converted to Top of Atmospheric (TOA) radiance by the following:

$$L_{TOA} = \frac{[L_{MAX} - L_{MIN}] \times DN}{MaxGray} + L_{MIN}, \quad (1)$$

where L_{TOA} is the spectral radiance at the sensor's aperture in $Wm^{-2}sr^{-1}\mu m^{-1}$, L_{MAX} and L_{MIN} are the maximum and minimum radiance values for a given band, $MaxGray$ is the maximum number of gray value and DN is the digital number for a given band. In addition, $0.31 Wm^{-2}sr^{-1}\mu m^{-1}$ must be subtracted from the calculated radiance to calibrate the result with that found from the ETM+ Thermal bands (Barsi *et al*, 2003a).

3.2 TOA Radiance to Surface Radiance

The surface radiance is then calculated using the RCE method. This procedure assumes that all pixels in a channel of the thermal infra-red band have the same emissivity constant, from which a surface radi-

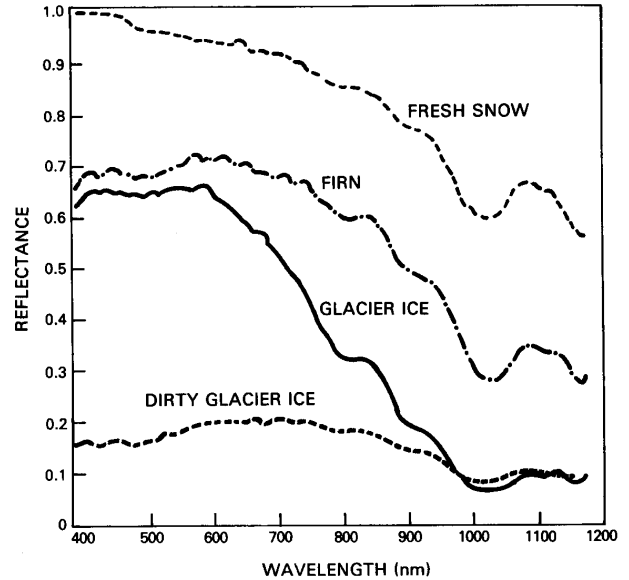


Fig. 3. Reflectance spectrum of snow and ice surfaces (Hall *et al*, 1985)

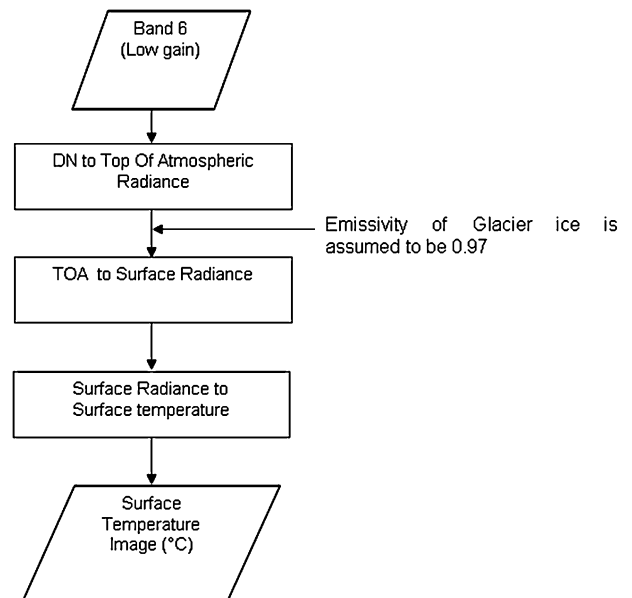


Fig. 4. Flow chart showing the methodology employed in this work

ance image is extracted. Removing the effect of the atmosphere in the thermal region is an essential step when using thermal band data for temperature studies. Knowing the properties of the atmosphere, a radiative transfer model can then be used to estimate the transmission, the upwelling and downwelling ra-

diances. Once these parameters are known, it is possible to convert the space-radiance to surface-leaving radiance. We make use of a web-based Atmospheric Correction Parameter Calculator (ACPC, http://landsat.gsfc.nasa.gov/atm_corr/) to estimate the site-

specific atmospheric transmission, upwelling and atmospheric path radiance, and downwelling or sky radiance. This tool uses the NCEP modelled atmospheric global profile for a particular date, time, latitude and longitude as input, along with MODTRAN

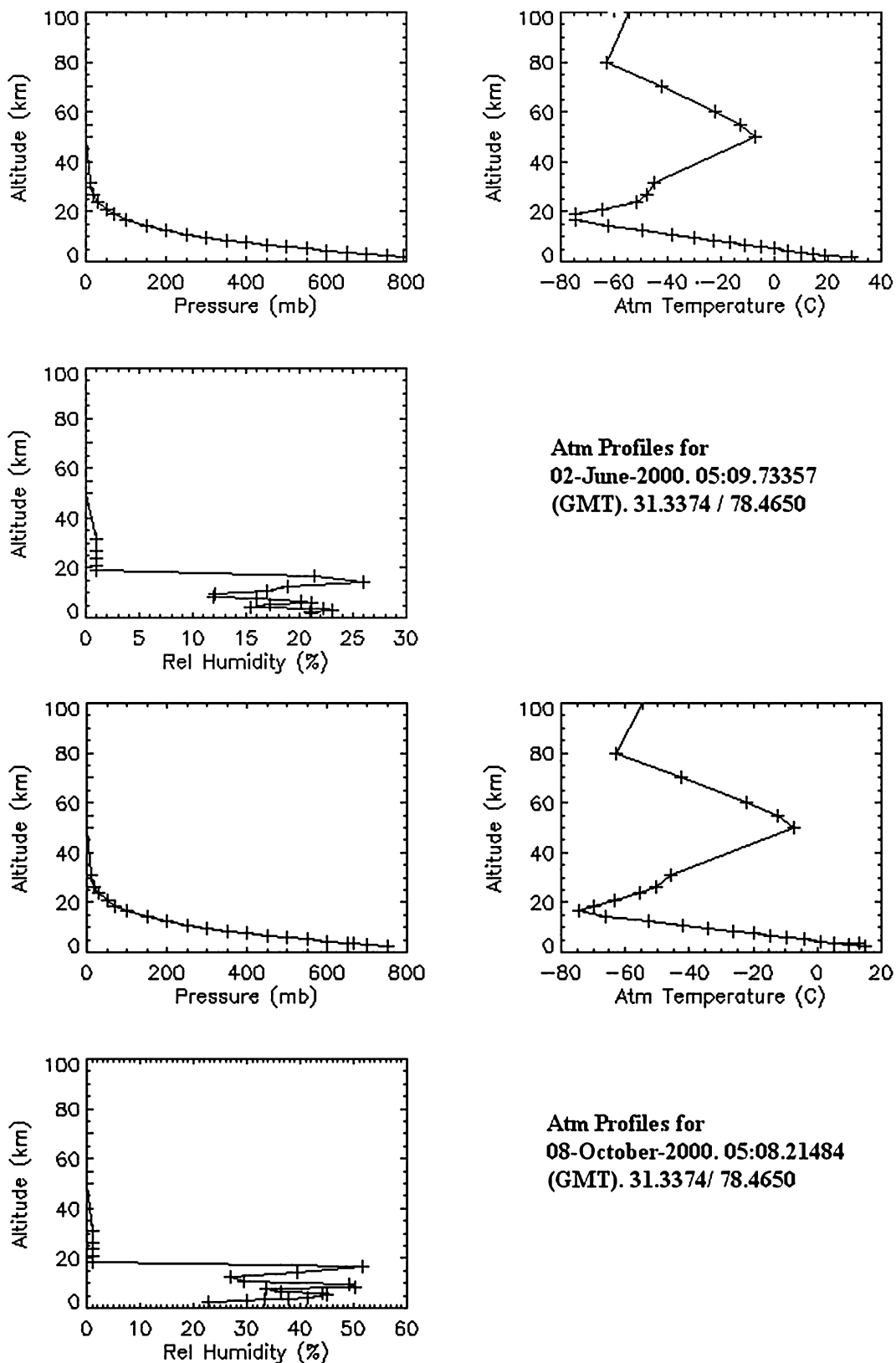


Fig. 5. Atmospheric profiles calculated using the Atmospheric Correction Parameter Calculator for (a) the scene dated 02-June-2000 and (b) the scene dated 08-October-2000.

Table 2. Atmospheric parameters calculated for use in eq. (2) using the Atmospheric Correction Parameter Calculator

Sl. No.	Scene Date	Scene centre Latitude/Longitude (DD)	Atmospheric Transmission	Upwelling W/(m ² . sr. μm)	Downwelling W/(m ² . sr. μm)
1	2-June-2000	31.3374/78.4650	0.91	0.64	1.1
2	8-Oct-2000	31.3374/78.4650	0.92	0.52	0.89

software and a suite of integration algorithms. The conversion of TOA radiance to surface radiance is done using (Barsi *et al.*, 2003b):

$$L_T = \frac{L_{TOA} - L_U - \tau(1 - \epsilon) \times L_D}{\tau \times \epsilon}, \quad (2)$$

where L_T is the radiance of a blackbody target of temperature T Kelvin (surface radiance), L_{TOA} is the TOA spectral radiance calculated using eq. (1), τ is the atmospheric transmission at the sensor's aperture, ϵ is the surface emissivity, L_U is the upwelling spectral radiance between the surface and the sensor (in $\text{Wm}^{-2} \text{sr}^{-1} \mu\text{m}^{-1}$) and L_D is the downwelling spectral radiance from the sky ($\text{Wm}^{-2} \text{sr}^{-1} \mu\text{m}^{-1}$).

Assuming the emissivity of glacier ice to be 0.97, the surface radiance of the image is estimated, with the scene's centre used to calculate the parameters required for eq. (2). The atmospheric profiles created and the parameters calculated using the ACPC are shown in Figure 5 and Table 2, respectively.

3.3 Surface Radiance to Surface Temperature

Surface radiance is finally converted to surface temperature by (Barsi *et al.*, 2003a):

$$T = \frac{K_2}{\ln \left[\frac{K_1 + 1}{L_T} \right]}, \quad (3)$$

where T is the surface temperature in Kelvin, K_1 and K_2 are pre-launch calibration constants (666.09 and 1282.71, respectively) and L_T is the surface radiance from eq. (2). The temperatures are estimated in degrees Kelvin, and are then converted to degree Celsius by T (Kelvin)-273.15.

4. Results

The resulting surface temperatures for the two scenes are presented in Figures 6. The mean temperatures estimated for the area of interest are 17.25°C and 11.98°C for June and October, respectively. In the June scene (Figure 6a), the area that experiences temperatures lower than -5°C (black) is very small and mainly occur at some of the glacier boundaries, i.e. at the mountain peaks where a major proportion of the glaciers are in the $-5-0^\circ\text{C}$ (red) temperature range, covering the accumulation and part of the ablation

Table 3. Comparing Observed and retrieved surface temperature data

Date	Field Observed Temperature (°C)	Retrieved Temperature (°C)
02-06-2000	21°C	22.99°C
08-10-2000	16°C	17.41°C

areas. The remaining ablation area and snout regions show temperatures ranging from $0-5^\circ\text{C}$ (green). Lateral moraines can be demarcated by the linear nature of the areas showing a temperature range of $5-10^\circ\text{C}$ (blue), while the remaining portion of the basin is characterised by temperatures ranging between $10-30^\circ\text{C}$ (magenta and yellow), representing the non-glaciated areas and the Baspa River.

In the October scene (fig.6b), a greater proportion of the area shows temperatures lower than -5°C (black) (Figure 6b), including all glaciers (covering some 60% of the total area), with the remaining ablation area and snout regions having temperatures ranging from $-5-0^\circ\text{C}$ (red). A very small portion of the study area shows temperatures between $0-10^\circ\text{C}$ (green and blue), with the remaining part of the basin again characterised by a temperature range of $10-30^\circ\text{C}$ (magenta and yellow).

The surface temperature data from Sangla, and the retrieved average values are given in Table 3. We found a good correlation between the retrieved and observed values. In both season a difference of $1-2^\circ\text{C}$ is observed, however due to lack of availability of data more comparison could not be done. Again the results were compared with NCEP modelled mean daily skin temperature (surface temperature) provided by the NOAA-CIRES Climate Diagnostic Center, Boulder, Colorado, from their website at <http://www.cdc.noaa.gov/> for the same period. For June -02-2000 the mean surface temperature averaged for the day was 10.52°C for the same areal extent, with a difference of about 7°C . For October-08-2000, the mean surface temperature averaged for the day was found to be 7.41°C , a difference of about 5°C .

5. Conclusions

Global climate change has a significant impact on glaciers, which are very sensitive to changes in atmos-

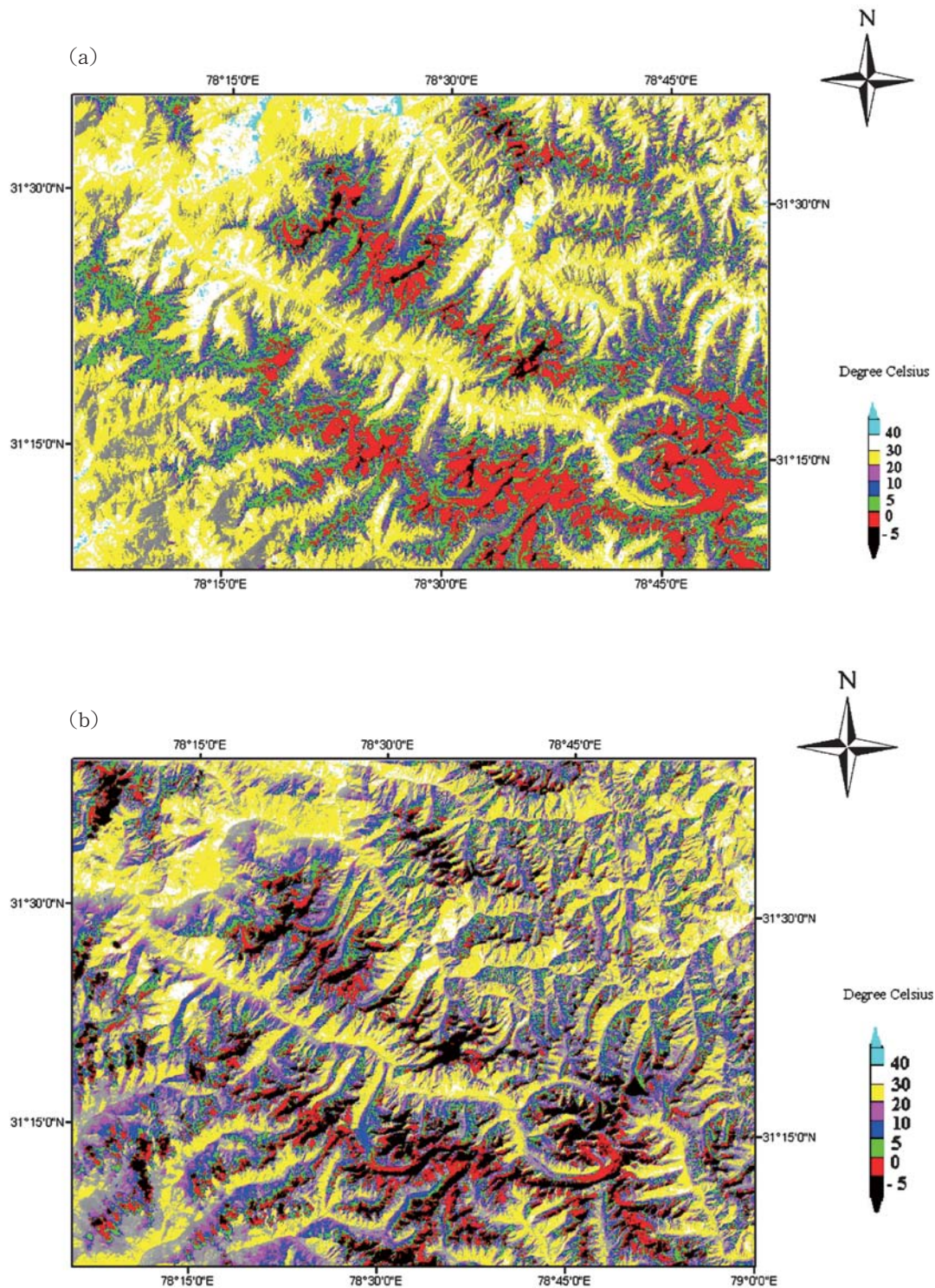


Fig. 6. Distribution patterns of the effective temperatures derived from the ETM+ band 6 (Low gain) scenes for 02-June-2000 (a) and 08-October-2000 (b).

pheric conditions. Consecutive temperature observations over the glaciated terrains of the Himalaya can therefore provide a clear understanding of climate change in this area. For example, a systematic analysis of thermal data from June to September may give a picture of the extent of the snowline at higher altitudes, which is one of the major inputs for the accurate estimation of the mass balance of glaciers when applying the accumulation area ratio (AAR)

method. In addition, the mapping of glacier landscapes can be enhanced using temperature data by the demarcation of debris cover, moraines, glacier boundaries, snow lines, and of course the accumulation and ablation zones. The main objective of this study was to examine a methodology for the estimation of surface temperatures from satellite data. The resulting extracted surface temperatures were compared to field data available for one location and the

results showed a good correlation. A difference of 1–2°C was observed between the temperatures obtained from the field and the retrieved data. The retrieved surface temperatures were again compared with daily average mean surface temperatures modelled by the NCEP. The NCEP modelled temperature was found to be 5–7°C cooler than the extracted surface temperature, which is a realistic expectation. The present results show that satellite data can provide regionally representative values for surface temperatures, which is not possible from ground observations given the scarcity of data. The derived surface temperature values are thus useful for studying changes in the regional climate over the Himalaya. However, to evaluate the accuracy of these results, more field data needs to be collected to obtain a higher degree of confidence in the estimations.

Acknowledgments

Special thanks to G. Chander, Science Applications International Corporation (SAIC), USGS, Earth Resources Observation and Science (EROS), USA and Dr. G. Philip, Wadia Institute of Himalayan Geology, India for fruitful suggestions and the Global Land Cover facility (GLCF), University of Maryland, USA for providing the Landsat ETM+ data, the HPSEB for providing the temperature data for Sangla and NOAA-CIRES for providing the surface temperature data. Modifications suggested by the anonymous referee and Dr. Yamazaki Takeshi have greatly improved the manuscript.

References

- Barsi, J.A., Schott, J.R., Palluconi, F.D., Helder, D.L., Hook, S. J., Markham, B.L., Chander, G. and O'Donnell, E.M. (2003a): Landsat TM and ETM+ thermal band calibration, *Canadian Journal of Remote Sensing*, **29** (2), 141–153.
- Barsi, J.A., Barker, J.L. and Schott, J.R. (2003b): An Atmospheric Correction Parameter Calculator for a Single Thermal Band Earth-Sensing Instrument. IGARSS03, 21–25 July 2003, Centre de Congres Pierre Baudis, Toulouse, France, 3.
- Dyrurgerov, M., (2003): Mountain and sub polar glaciers show an increase in sensitivity to climate warming and intensification of the water cycle. *Journal of Hydrology*, **282**, 164–176.
- Hall, D.K. and Martinec, J. (1985): *Remote sensing of ice and snow*. Chapman and Hall, New York, 189pp.
- IPCC (2001). Climate Changes 2001: The Scientific Basis.(2003): Contribution of Working Group I to the Third Assessment Report of the Intergovernmental Panel on Climate Change (Houghton, J.T., Y. Ding, D.J. Griggs, M. Noguer, P.J. van der Linden, X. Dai, K. Maskell and C.A. Johnson (eds) Cambridge University Press, Cambridge, United Kingdom and New York, NY, USA, 881.
- Kaser, G., Gogley, J., Dyrurgerov, M., Meier, M., and Ohmura, A.(2006): Mass balance of glaciers and ice caps: Consensus estimates for 1961–2004. *Geophysical Research Letters*, **33** (L19501), 10.1029/2006GL027511.
- Kulkarni, A.V. (1991): Glacier inventory in Himachal Pradesh using satellite data. *Journal of the Indian Society of Remote Sensing*, **19** (3), 195–203.
- Kulkarni, A.V. and Bahuguna, I.M. (2002a): Glacial retreat in the Baspa basin, Himalaya, monitored with satellite stereo data, Correspondence, *Journal of Glaciology*, **48** (160), 171–172.
- Kulkarni, A.V., Mathur, P., Rathore, B.P., Alex, Suja, Thakur, N. and Manoj Kumar (2002b): Effect of global warming on snow ablation pattern in the Himalaya. *Current Science*, **83** (2), 120–123.
- Kulkarni, A.V., Rathore, B.P. and Alex, Suja (2004): Monitoring of glacial balance in the Baspa basin using accumulation area ratio method. *Current Science*, **86** (1), 185–190.
- Kulkarni, A.V., Rathore, B.P., Mahajan, S. and Mathur, P. (2005): Alarming retreat of Parbati Glacier, Beas basin, Himachal Pradesh. *Current Science*, **88** (11), 1844–1850.
- Kulkarni, Anil V., Dhar, Sunil, Rathore, B.P., Babu Govindha Raj, K. and Kalia, Rajeev (2006): Recession of Samudra Tapu Glacier, Chandra River Basin, Himachal Pradesh. *Journal of the Indian Society of Remote Sensing*, **34** (1), 39–46.
- Philip, G. and Ravindran, K.V. (1998): Glacial Mapping using Landsat Thematic Mapper Data: A case study in parts of Gangotri Glacier, NW Himalaya. *Journal of the Indian Society of Remote Sensing*, **26**, 29–34.
- Philip, G. and Sah, M.P. (2004): Mapping Repeated Surges and Retread of Glaciers Using IRS-1C/1D Data: A Case Study of Shaune Garang Glacier, Northwestern Himalaya. *International Journal for Applied Earth Observation and Geoinformation*, **6** (2), 127–141.
- Raina, V.K. (2005): Status of Glacier Studies in India, *Himalayan Geology*, **26** (1), 285–293.
- Rignot, E. and Kanagaratnam, P. (2006): Changes in the velocity structure of the Greenland Ice Sheet, *Science*, **311**, 986–990.
- Smith, L., Sheng, Y., Forster, R., Steffen, K., Frey, K. and Alsdorf, D. (2003): Melting of small Arctic ice caps observed from ERS scatterometer time series, *Geophysical Research Letters*, **30** (20), 10.1029/2003GL017641.
- WWF Nepal Program (2005): An overview of Glaciers, Glacier Retreat, and Subsequent Impacts in Nepal, India and China, Compiled by Joe Thomas K and Sandeep Chamling Rai, 70.